

## Magnetic stability of ultrathin FeRh films

G. C. Han, J. J. Qiu, Q. J. Yap, P. Luo, D. E. Laughlin et al.

Citation: *J. Appl. Phys.* **113**, 17C107 (2013); doi: 10.1063/1.4794980

View online: <http://dx.doi.org/10.1063/1.4794980>

View Table of Contents: <http://jap.aip.org/resource/1/JAPIAU/v113/i17>

Published by the [American Institute of Physics](#).

---

### Related Articles

The low-frequency alternative-current magnetic susceptibility and electrical properties of Si(100)/Fe<sub>40</sub>Pd<sub>40</sub>B<sub>20</sub>(X Å)/ZnO(500Å) and Si(100)/ZnO(500Å)/Fe<sub>40</sub>Pd<sub>40</sub>B<sub>20</sub>(YÅ) systems

*J. Appl. Phys.* **113**, 17B303 (2013)

Interface-controlled magnetism and transport of ultrathin manganite films

*J. Appl. Phys.* **113**, 17C711 (2013)

First observation of magnetoelectric effect in M-type hexaferrite thin films

*J. Appl. Phys.* **113**, 17C710 (2013)

Magnetic and structural properties of (Ga,Mn)As/(Al,Ga,Mn)As bilayer films

*Appl. Phys. Lett.* **102**, 112404 (2013)

Strain effects in epitaxial Mn<sub>2</sub>O<sub>3</sub> thin film grown on MgO(100)

*J. Appl. Phys.* **113**, 17A314 (2013)

---

### Additional information on *J. Appl. Phys.*

Journal Homepage: <http://jap.aip.org/>

Journal Information: [http://jap.aip.org/about/about\\_the\\_journal](http://jap.aip.org/about/about_the_journal)

Top downloads: [http://jap.aip.org/features/most\\_downloaded](http://jap.aip.org/features/most_downloaded)

Information for Authors: <http://jap.aip.org/authors>

## ADVERTISEMENT



**AIP Advances**

Now Indexed in Thomson Reuters Databases

Explore AIP's open access journal:

- Rapid publication
- Article-level metrics
- Post-publication rating and commenting

## Magnetic stability of ultrathin FeRh films

G. C. Han,<sup>1,a)</sup> J. J. Qiu,<sup>1</sup> Q. J. Yap,<sup>1</sup> P. Luo,<sup>1</sup> D. E. Laughlin,<sup>2</sup> J. G. Zhu,<sup>2</sup> T. Kanbe,<sup>3</sup> and T. Shige<sup>3</sup>

<sup>1</sup>Data Storage Institute, A\*STAR, Republic of Singapore

<sup>2</sup>Data Storage Systems Center, Carnegie Mellon University, Pittsburgh, Pennsylvania 15213, USA

<sup>3</sup>Showa Denko K.K., 13-9, Shiba daimon 1-Chome, Minato-ku, Tokyo 105-8518, Japan

(Presented 17 January 2013; received 4 November 2012; accepted 3 December 2012; published online 21 March 2013)

This paper presents magnetic properties of highly ordered ultrathin FeRh films deposited on Si/SiO wafers with MgO as a buffer layer. The antiferromagnetic to ferromagnetic (FM) transition is observed with a thickness as low as 3 nm. However, as the thickness decreases, the residual magnetization ( $M_{rs}$ ) at low temperature increases and the amplitude of the transition decreases. In addition, the transition becomes much broader for the thinner films. This broadening is related to the grain size reduction in the thinner films. The temperature dependence of the magnetization of a highly ordered B2 FeRh film with a thickness of 10 nm was carefully measured as a function of field. The results show that the transition temperature decreases almost linearly with a rate of 0.93 K/kOe (heating) and 0.97 K/kOe (cooling) close to the value for the bulk samples, while  $M_{rs}$  obtained at 100 K increases rapidly at low field and then linearly at a field larger than 10 kOe, which clearly demonstrates that an applied field would induce FM stabilization in ultrathin FeRh films. © 2013 American Institute of Physics. [<http://dx.doi.org/10.1063/1.4794980>]

FeRh films have been attracting much interest for their potential applications in magnetic memory<sup>1,2</sup> and recording media.<sup>3</sup> For these applications, FeRh film is used to reduce the switching field of the storage layer through the exchange coupling between the ferromagnetic (FM) FeRh layer and the storage layer at elevated temperatures without sacrificing the thermal stability of the storage layer at ambient temperature, since the antiferromagnetic (AF) FeRh layer provides negligible exchange coupling to the storage layer. The major challenge is to prepare ultrathin FeRh films with a single AF phase at ambient temperature, which will convert to the FM phase at elevated temperatures, and vice versa. So far, a sharp AF-FM transition of FeRh film was only reported at a thickness above 14 nm.<sup>4</sup> For ultrathin films with a thickness of 10 nm or below, a large residual magnetization ( $M_{rs}$ ) is generally observed.<sup>5</sup> The origin of this low temperature FM phase remains unclear. Fan *et al.*<sup>6</sup> observed the existence of a FM phase in a region within 6–8 nm near the top and bottom interfaces of a FeRh film. Based on *ab initio* calculations, Lounis *et al.*<sup>7</sup> found that a FM state is stable up to 9 atomic layers for Rh-terminated FeRh films. In addition, the AF structure would become unstable when the amount of the site-exchange defect density exceeds a threshold of 0.8%/f.u.<sup>8</sup> Furthermore, based on the phase diagram,<sup>9</sup> the AF to FM transition can be only achieved in the  $\alpha''$  phase which is formed within a narrow Fe atomic concentration range from 45% to 51%. Due to slow diffusion rate of Rh, it is likely that a mixture of the FM Fe-rich  $\alpha'$  phase and the paramagnetic Rh-rich  $\gamma$  phase is formed in the film. In this paper, the magnetic stability of ultrathin ( $\leq 10$  nm) FeRh films is examined. It is found that for such

ultrathin FeRh films, the low temperature FM stabilization is sensitive to the film thickness and the applied magnetic field. An AF to FM transition is observed at a thickness as low as 3 nm, which is close to the FM stabilization thickness based on *ab initio* calculations for Rh-terminated film.<sup>7</sup>

FeRh films were grown on thermally oxidized Si wafers with MgO buffer layer by co-sputtering from pure Fe and Rh targets. The composition was adjusted by controlling the sputtering power of each target. The deposition pressure and temperature used are 0.059 Pa and 650 °C, respectively. The films were capped by a 5 nm thick Ru layer to prevent oxidation of the FeRh layer. The top surface profiles were characterized by using atomic force microscope (AFM). The crystalline structures of all FeRh films were analyzed by x-ray diffraction (XRD) and show highly order B2 phase. Magnetic properties were measured using a superconducting quantum interference device (SQUID) with a maximum field and temperature of 70 kOe and 400 K, respectively.

Figs. 1(a) and 1(b) show temperature dependence of magnetization (M-T) for various thicknesses in the presence of a magnetic field of 1 kOe and 50 kOe, respectively. As the thickness decreases,  $M_{rs}$  increases and the amplitude of the magnetization transition decreases. In addition, the transition temperature shifts to lower temperatures for the thinner films. This implies that in these ultrathin films, the lattice mismatching induced stress (compression) should not be a dominant factor for the FM phase formation, since the compression should delay the onset of AF-FM transition, i.e., there should be an increase in the transition temperature instead of the decrease seen here. The AF-FM transition is observed at a thickness as low as 3 nm, which is the lowest thickness for the observation of the transition reported so far. This thickness is also close to the theoretical thickness limit

<sup>a)</sup>Author to whom correspondence should be addressed. Electronic mail: han\_guchang@dsi.a-star.edu.sg.

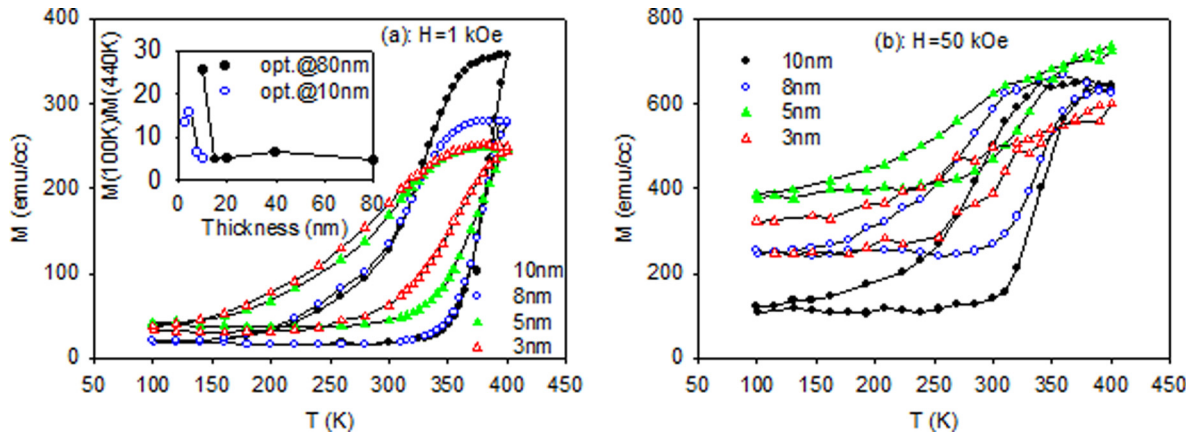


FIG. 1. Temperature dependence of magnetization as a function of film thickness measured at an applied field of 1 kOe (a) and 50 kOe (b). The inset in (a) gives the ratio of the residual magnetization at 100 K to the magnetization at 400 K for various thicknesses, where the filled and open circles give the data for the films with the composition optimized at the thickness of 80 nm and 10 nm, respectively.

for the stable AF phase based on *ab initio* studies.<sup>7</sup> The AF-FM transition is not yet completed when the sample is heated up to 400 K at 1 kOe. When a field of 50 kOe was applied, the transition is shifted below 400 K. As a result, the larger magnetic transition can be obtained and the magnetization at 400 K is much larger than that measured at 1 kOe. Accordingly,  $M_{rs}$  also increases significantly. This magnetization increase is not caused from the shift of the AF-FM transition towards the lower temperature at a higher field, but the field-induced FM stabilization. As shown in Fig. 1(b), for thickness of 10 nm and 8 nm and at a field of 50 kOe, the AF-FM transitions take place at temperatures higher than 200 K and the FM-AF transitions are also completed at about 120 K. This field-induced FM stabilization is further enhanced as the thickness decreases except for the 3 nm thick film, for which a residual magnetization lower than that of the 5 nm thick film is observed. An irreversible increase in  $M_{rs}$  was also observed after one cycle of heating and cooling at 50 kOe. It should be pointed out that as the thickness decreases below 5 nm, the magnetization change seems to become unstable at 50 kOe with much broader transition observed. The magnetization keeps increasing with temperature even after the AF-FM transition. In contrast, for 8 nm thick FeRh film, there is a well-defined AF-FM transition at a temperature lower than that of the 10 nm thick film and the magnetization starts to decrease immediately after the transition. To understand the origin of the residual magnetization, the inset of Fig. 1(a) shows the ratio of  $M_{rs}$  at 100 K to the maximum magnetization achieved at 400 K as a function of thickness. The data for thickness exceeding 10 nm (filled circles) were obtained from a series of samples, whose composition is first tuned to give the lowest  $M_{rs}$  at a thickness of 80 nm through adjusting the sputtering power of Fe and Rh targets. It is found that this composition results in a large  $M_{rs}$  when the thickness is reduced to 10 nm. By further tuning the composition at a fixed thickness of 10 nm, an even smaller  $M_{rs}$  (open circles) was achieved. As shown in the inset, the  $M_{rs}$  ratio remains unchanged at about 4.5% down to 10 nm. This result implies that  $M_{rs}$  above 10 nm is not from film thickness dependent stress, but from composition fluctuations over the film. On the other hand, the significant

increase of the  $M_{rs}$  ratio below 10 nm is most likely due to an increase of the interfacial FM phase in the samples as reported by Ding *et al.*<sup>10</sup> and Baldasseroni *et al.*<sup>11</sup>

Fig. 2 shows the magnetization curves of the same samples measured at 300 K. It is obvious that these ultrathin films show soft FM behaviour with a small coercivity. Magnetization saturates at a field of less than 500 Oe. The inset of Fig. 2 gives the saturation magnetization ( $M_s$ ) of the films obtained at 100 K and 300 K. At 300 K,  $M_s$  increases monotonously as the thickness decreases from 10 nm to 3 nm, while at 100 K, there is a slight decrease in  $M_s$  when the thickness is reduced from 5 nm to 3 nm. The larger  $M_s$  observed at 300 K in the 3 nm thick film is due to the lower AF-FM transition temperature as shown in Fig. 1(a), while the lower  $M_s$  at 100 K is probably from the instability of the FM phase in the 3 nm thick film. However, in the presence of a high field, the magnetization of the 3 nm thick film becomes unstable. As can be seen from Fig. 1(b), the magnetization at 50 kOe is much smaller for the 3 nm thick film than that of the 5 nm thick films, while a similar magnetization is obtained at a field of 1 kOe.

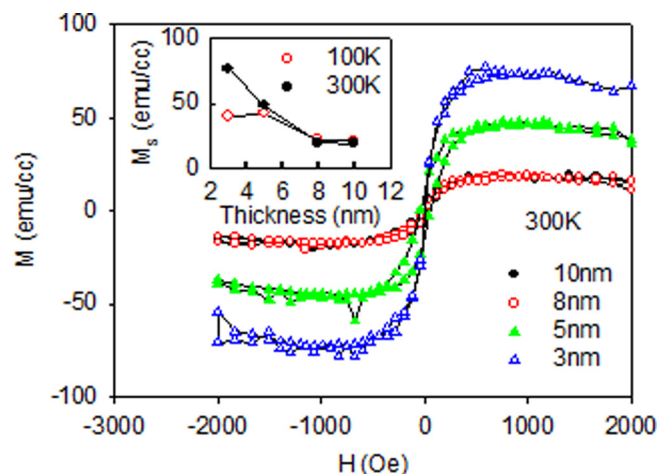


FIG. 2. Magnetization curves measured at 300 K for various thicknesses, showing large residual magnetization increase when the film thickness is reduced to less than 8 nm. The inset gives the saturation magnetization ( $M_s$ ) obtained at 100 K and 300 K, showing different  $M_s$  variations when the film thickness is reduced from 5 nm to 3 nm.

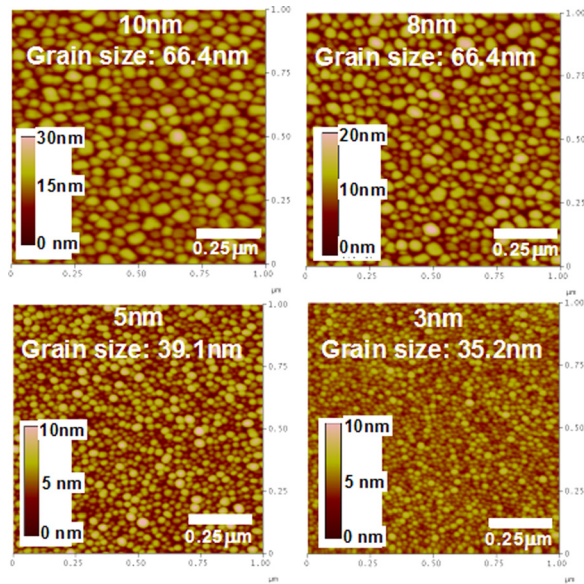


FIG. 3. AFM images for FeRh films with different thicknesses, showing significant reduction in grain size when the film thickness is reduced from 8 nm to 5 nm.

As shown in Fig. 1 the transition becomes significantly broadened as the thickness decreases from 8 nm to 5 nm. To understand the mechanism of the broadening, Fig. 3 shows the AFM images of surface morphology. The grain sizes measured for different samples are also given in the figure. When the thickness decreases from 8 to 5 nm, the grain size decreases significantly from 66.4 nm to 39.1 nm which corresponds to the significant increase in the transition width and  $M_{rs}$  as shown in Fig. 1. This can be understood from the surface/interface effect as the surface area increases with decrease of the grain size. This result is in agreement with that reported for thicker films.<sup>12</sup>

It was reported<sup>12,13</sup> that FM nucleation is favoured in the presence of a magnetic field. As a result, the magnetic transition is shifted to lower temperature under a higher field, which is confirmed in Fig. 1. In order to explore the mechanism of the formation of field-induced FM phase at low temperature, the field dependence of M-T curves of the 10 nm thick FeRh film was obtained. To avoid data crowding, Fig. 4 only shows the transition temperature and the  $M_{rs}$  at 100 K as a function of magnetic field. The transition temperature ( $T_{tr}$ ) is defined as the temperature at which the derivative of M-T curves in the AF-FM and FM-AF transitions is maximum. The field coefficient of transition temperature  $dT_{tr}/dH$  is 0.93 and 0.97 K/kOe for heating and cooling, respectively, which is close to 1 K/kOe and 0.8 K/kOe reported by Ohtani and Hatakeyama<sup>12</sup> and Maat *et al.*<sup>13</sup> for FeRh thick films, respectively, and 0.82 K/kOe reported by Kouvel<sup>14</sup> for the bulk FeRh alloys. This result implies that the field-induced transition shift is intrinsic for the AF phase, independent of the thickness and composition. This is in contrast to the residual magnetization, which is sensitive to the composition, stress, defect, thickness as well as field. As shown by the open circle/square symbols,  $M_{rs}$  increases rapidly when the field increases from 0.5 kOe to 10 kOe, then increases almost linearly with the field. This field-induced ferromagnetism appears reversible upon the thermal cycle at low

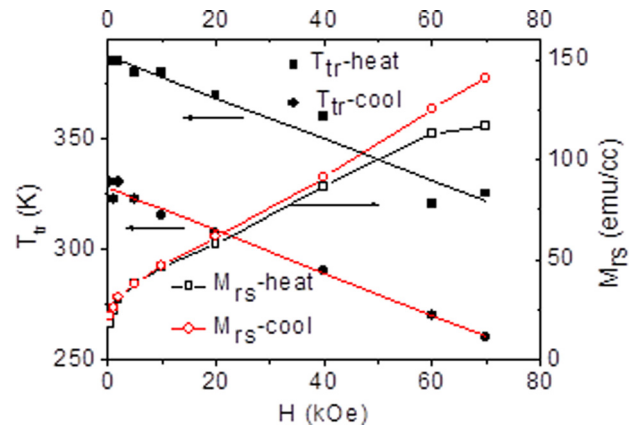


FIG. 4. Transition temperature ( $T_{tr}$ ) and residual magnetization ( $M_{rs}$ ) at 100 K as a function of magnetic field, showing a linear shift of the transition temperature and the field-induced ferromagnetic stability.

fields and then becomes irreversible when the field is larger than 10 kOe. The amount of increased  $M_{rs}$  increases as the field increases. This could be attributed to the possibility of the field driving the FM-AF transition of some AF phases to a temperature below 100 K. It is worth mentioning that even at such a thickness of 10 nm, our sample shows a low  $M_{rs}$ , having a magnetization value of about 18 emu/cc at 100 K in the presence of 0.5 kOe, in contrast to 250 emu/cc reported by Suzuki *et al.*<sup>5</sup> However, we also noted that the maximum magnetization value ( $\sim 670$  emu/cc) measured in the FM state is much lower than the bulk value. This magnetization reduction is ascribed to the grain size induced FM instability and the magnetic moment reduction of Fe and Rh spins at the interface.

In conclusion, small residual FM phase is observed for ultrathin FeRh films deposited on Si wafer. The AF phase becomes more and more unstable as the thickness decreases. The FM phase could be stabilized by a magnetic field when the FeRh film thickness is reduced below 10 nm. Although the shift of the overall AF-FM transition to lower temperatures as observed under increasing magnetic field is intrinsic for FeRh alloys, the field-induced FM phase is closely related to the film thickness, composition, and other extrinsic conditions.

This work was supported by Showa Denko, the Data Storage Systems Center of Carnegie Mellon University and Data Storage Institute of A\* STAR, Singapore.

- <sup>1</sup>E. Fullerton, S. Maat, and J. U. Thiele, U.S. patent 20 050281 081 (2005).
- <sup>2</sup>J.-G. Zhu, Y. Luo, and X. Li, U.S. patent 7,826,258 (2010).
- <sup>3</sup>J. Thiele, S. Maat, and E. E. Fullerton, *Appl. Phys. Lett.* **82**, 2859 (2003).
- <sup>4</sup>D. Kande *et al.*, *IEEE Trans. Magn.* **47**, 3296 (2011).
- <sup>5</sup>I. Suzuki *et al.*, *J. Appl. Phys.* **105**, 07E501 (2009).
- <sup>6</sup>R. Fan *et al.*, *Phys. Rev. B* **82**, 184418 (2010).
- <sup>7</sup>S. Lounis, M. Benakki, and C. Demangeat, *Phys. Rev. B* **67**, 094432 (2003).
- <sup>8</sup>Y. Kaneta *et al.*, *Jpn. J. Appl. Phys., Part 1* **50**, 105803 (2011).
- <sup>9</sup>T. B. Massalski, *Binary Alloy Phase Diagrams* (ASM International, Materials Park, OH, 1992), Vol. 2, p. 1760.
- <sup>10</sup>Y. Ding *et al.*, *J. Appl. Phys.* **103**, 07B515 (2008).
- <sup>11</sup>C. Baldasseroni *et al.*, *Appl. Phys. Lett.* **100**, 262410 (2012).
- <sup>12</sup>Y. Ohtani and I. Hatakeyama, *J. Magn. Magn. Mater.* **131**, 339 (1994).
- <sup>13</sup>S. Maat *et al.*, *Phys. Rev. B* **72**, 214432 (2005).
- <sup>14</sup>J. S. Kouvel, *J. Appl. Phys.* **37**, 1257 (1966).